

Dislocation Mobility and Anomalous Shear Modulus Effect in ^4He Crystals

Abdul N. Malmi-Kakkada · Oriol T. Valls · Chandan Dasgupta

March 6, 2024

Abstract We calculate the dislocation glide mobility in solid ^4He within a model that assumes the existence of a superfluid field associated with dislocation lines. Prompted by the results of this mobility calculation, we study within this model the role that such a superfluid field may play in the motion of the dislocation line when a stress is applied to the crystal. To do this, we relate the damping of dislocation motion, calculated in the presence of the assumed superfluid field, to the shear modulus of the crystal. As the temperature increases, we find that a sharp drop in the shear modulus will occur at the temperature where the superfluid field disappears. We compare the drop in shear modulus of the crystal arising from the temperature dependence of the damping contribution due to the superfluid field, to the experimental observation of the same phenomena in solid ^4He and find quantitative agreement. Our results indicate that such a superfluid field plays an important role in dislocation pinning in a clean solid ^4He at low temperatures and in this regime may provide an alternative source for the unusual elastic phenomena observed in solid ^4He .

Abdul N. Malmi-Kakkada · Oriol T. Valls
School of Physics and Astronomy, University of Minnesota, Minneapolis, Minnesota 55455
E-mail: otvalls@umn.edu
Present address: of Abdul N. Malmi-Kakkada
Dept. of Chemistry, University of Texas at Austin,
105 E 24th St, Austin, TX 78712

Chandan Dasgupta
Centre for Condensed Matter Theory, Department of Physics, Indian Institute of Science,
Bangalore 560012, India

1 Introduction

Solid ^4He is the archetype of a quantum crystal. Quantum effects in solid ^4He were pointed out as early as 1960s [1, 2], and extensive work on this and many other aspects of its properties [3] has been subsequently performed. Among the quantum mechanical effects it exhibits are those associated with crystalline defects. More recently, the observation of a marked period drop with temperature in torsional oscillator experiments [4, 5] in solid ^4He , originally interpreted as evidence for a “supersolid” state, renewed both theoretical and experimental interest on topics related to quantum crystals. Subsequently, solid ^4He was also shown to undergo an anomalous softening of the shear modulus [6, 7]. This drop in the shear modulus was observed at the same temperature range as the drop in period seen in torsional oscillator experiments. These results suggested that the anomalous shear modulus effect, rather than the change in the inertial mass dragged by the oscillator, was responsible for the observed drop in torsional oscillator period [8, 9]. Nevertheless, the discovery of this anomalous shear modulus softening has led to new and important questions being posed on the elastic properties of solid ^4He and in particular on the role of dislocation lines in this material. Given that the mechanical properties of crystals are largely dictated by dislocation lines, the observed anomalous shear modulus behavior can provide fundamental insights into the elastic properties of quantum crystals. That is, some of the features associated with the behavior of the dislocation lines in solid ^4He crystal may be due to quantum crystal effects and therefore not be ordinarily observed in classical crystals.

Indeed, the reasons for the anomalous shear modulus behavior in solid ^4He are still much debated. A frequently held position is simply that dislocation lines are pinned by ^3He impurities at low temperatures but become mobile (able to glide) at higher temperatures when impurities are no longer able to pin the dislocation network [6]. The experimentally observed dependence of the elastic anomaly on ^3He concentration suggests that impurities play an important role in this phenomenon. Other proposals [9, 10, 11] model dislocation lines as vibrating strings unable to execute free glide motion. String-like bowing of such dislocation lines in response to stress is taken into account in explaining the shear modulus behavior. Yet another proposal [12, 13] attempts to model the shear modulus behavior by taking into account the interactions between dislocation lines as well as the Peierls barrier contribution to the damping of the dislocation motion.

The role that quantum phenomena may play in the anomalous elastic behavior is disputed. The effect that a putative quantum field associated with dislocation lines could play in the anomalous shear modulus behavior has been recently explored in the literature [14]. Quantum Monte Carlo calculations [15, 16] have shown that superfluidity can occur in dislocation cores. A recent experimental study raised the possibility that dissipative mass flux in solid ^4He could be associated with superfluid cores of edge dislocations [17]. Thus, the question of the presence of superfluid field in solid ^4He has become controversial, as seen on the one hand from the several models mentioned above,

that seek to explain the anomalous shear modulus effect without invoking the presence of a superfluid field, and on the other by numerous other studies [14, 18, 19] which take into account, or discuss the possibility of [20, 21, 22, 23, 24] the presence of a superfluid field. Therefore, it seems to us highly pertinent to investigate the effect of an assumed superfluid field on dislocation motion within crystalline ^4He .

Given this context of exploring the role that superfluidity may play in solid ^4He , we begin by examining the possible effects of an assumed superfluid field on its elastic properties via a novel calculation of the dislocation mobility in a quantum crystal. Assuming a minimal coupling [25] between the dislocation line strain and the superfluid field it is in principle possible for the superfluid field either to make it easier for the dislocation line to move or to contribute to the pinning of the dislocation line, making it harder for it to move. A prior study of the interplay of dislocation lines and superfluid field showed that a quenched dislocation line enhances superfluidity near it while moving dislocation lines can suppress superfluidity in its vicinity [26]. The results of our calculation of dislocation motion damping arising from an assumed superfluid field associated with the dislocation line, lead us to investigate the possibility that at low temperatures and in low impurity crystals, such damping may play an important role in pinning the dislocation motion and therefore affect the shear modulus behavior. At low temperatures, we would expect quantum effects other than thermal phonon scattering and impurity pinning to be more important in terms of damping of dislocation line motion and the associated anomalous shear modulus behavior. Experimental studies of ultra pure solid ^4He samples with negligible concentration of ^3He impurities also exhibit anomalous shear modulus behavior [27, 28]. For ^4He crystals characterized by distances between ^3He impurity atoms larger than the cell size in which ^4He is contained, anomalous shear softening is reported [29]. High quality ^4He crystals presumably with low impurity concentration, also exhibit anomalous shear modulus behavior [30]. These experimental observations inevitably point out, as noted in Ref. [28], that dislocation pinning by impurities may not be the only mechanism responsible for anomalous shear modulus behavior.

In this paper, then, we explore the consequences, for the elastic properties of a quantum crystal, of assuming the existence of a superfluid field associated with the dislocation lines and examine its relation to the sharp decrease of the shear modulus with temperature observed in experimental studies [11, 31, 30]. As a first step we study the effect of the superfluid field on dislocation motion, i.e. we investigate the damping of dislocation line motion. To do so, we calculate the mobility of a gliding dislocation line, which in a conventional crystal corresponds to an inverse viscosity, in a quantum crystal. Our calculation of the dislocation motion mobility is performed by extending a well known procedure developed in earlier work on quasicrystals [32] to quantum crystals. We use a straightforward hydrodynamic approach: the hydrodynamic equations for ^4He crystals as developed in Refs. [2, 33]. Taking into account earlier studies [34, 35] on the role that dislocation lines play in determining the elastic

properties of solid ^4He crystal, we relate the contribution to the dislocation mobility produced by the assumed field, to the shear modulus of the crystal.

Obviously, this would be a purely abstract exercise unless we made contact with experiment: we can claim validity for our ideas only after showing that they provide at least an alternative explanation for known experimental facts. Therefore we then model existing shear modulus experimental data, [11,31,30] and show that the drop in shear modulus with increasing temperature is perfectly consistent with the existence of an underlying rapid increase of the superfluid order parameter as the temperature decreases. Our assumption of a superfluid field associated, not with bulk superfluidity but rather with the dislocation line cores, does not violate, as we shall see below, the present experimental upper limit on the possible superfluid fraction. We conclude that the damping of dislocation motion due to superfluid field is important, in the low temperature limit, to be considered with other sources of damping such as ^3He impurities and thermal phonon scattering.

The experiments [11,31,30] on the shear modulus behavior of solid ^4He use a procedure where a shear strain is applied on the crystal at a set frequency, ω . At the lower frequencies utilized in experimental studies (as low as 2 Hz for the applied strain), the experiments are best analyzed, in agreement with the arguments presented in Ref. [36], in the limit, where the inertial mass of the dislocation line can be ignored and one can, moreover, focus on the quasi-static limit [37] for the strain due to dislocation motion. At higher frequencies the possibility arises of a phase shift between the applied strain and the resultant displacement of the dislocation line. Although for the purposes of our study, we focus mainly on understanding the mechanism behind the sharp drop in shear modulus as a function of temperature for a gliding dislocation line, our model is amenable also to a higher frequency scenario where the dislocation executes some combination of gliding and string-like vibration, out of phase with the applied strain. Our procedure enables us, by making use of our results on dislocation pinning due to the superfluid field present within crystal ^4He , to model the low frequency shear modulus temperature behavior seen [6,7,38,11] in strain experiments as well as that [11,38] of the Q factor at higher frequencies.

The organization of the rest of this paper is as follows. In section 2 we present the hydrodynamic method used to calculate the mobility of a dislocation in a quantum solid, and show how the mobility can be related to the shear modulus. In section 3 we illustrate how our results can be used to model the experimental data on shear modulus softening in response to increasing temperature. Two figures illustrate the comparison between theory and experiment: very satisfactory agreement is found. Finally, section 4 contains a summary of the main results and concluding remarks.

2 Methods

2.1 Dislocation Mobility

We begin here by describing the method we use to calculate the dislocation mobility in a quantum crystal. This is based on an extension of the procedure [32] previously employed to compute the dislocation mobility in quasicrystals, combined with the usual hydrodynamic equations [2,33] for quantum crystals.

The considerations below are valid for both edge and screw dislocations. For illustrative purposes only, it is helpful to focus on edge dislocations. Consider such a dislocation with Burgers vector of length b in a crystal subjected to a shear stress σ . The shear stress will result in a force per unit length on the dislocation line, \mathbf{F}_D , which will cause the dislocation line to move. The velocity (\mathbf{V}_D) of the dislocation line [32] is then proportional to \mathbf{F}_D :

$$\mathbf{V}_D = M\mathbf{F}_D \quad (1)$$

where M is, by definition, the mobility coefficient and, for simplicity, we consider the vectors \mathbf{F}_D and \mathbf{V}_D to be parallel to each other. The general approach seen in [32] and [39] to the calculation of the mobility involves equating the rate of work done by a force applied on the dislocation line, which causes the line to move with a constant speed V_D , to the energy dissipation rate due to the fields associated with the dislocation line motion. Thus, one has,

$$F_D V_D = -\frac{d}{dt} \int d^2r E_{el}, \quad (2)$$

where the right hand side is the rate at which energy is dissipated in the elastic fields, as mentioned above, and the integral is over a two dimensional plane orthogonal to the dislocation line. The left hand side is the rate at which energy is transferred onto the dislocation line due to the applied force F_D .

To calculate the mobility, one isolates the terms in the right side of Eq. (2) that are proportional to V_D^2 . Then one extracts M from the relation:

$$F_D V_D = M^{-1} V_D^2, \quad (3)$$

where we have made use of Eq. (1). The left side of Eq. (3) is evaluated from the right side of Eq. (2) using hydrodynamic methods described below. Then, the constant of proportionality between the dissipation and the square of V_D is the inverse mobility of the dislocation line.

The contribution to the mobility of the dislocation line that we wish to calculate arises from physical phenomena at length scales much larger than the dislocation core size. A hydrodynamic description of superfluidity confined to narrow channels is valid whenever [40] the width of such channels exceeds the coherence length. Hence, it is valid in our case because the coherence length is of the order of interatomic distance, and the size of the typical superfluid region near the core of a dislocation line is [15,16] of order ~ 10 times the interparticle spacing or more. Hence, we can use the hydrodynamic methods

of Ref. [32]. The proper hydrodynamic approach in our case is as developed in Refs. [2, 33]. We particularly follow the notation of the latter.

We have for elastic energy density E_{el} and its differential, dE_{el} , the expressions:

$$\begin{aligned} dE_{el} &= Tds + \lambda_{ik}dw_{ik} + \phi d\rho + \mathbf{v}_n \cdot d\mathbf{g} + \mathbf{j}_s \cdot d\mathbf{v}_s, \\ E_{el} &= -P + Ts + \lambda_{ik}w_{ik} + \phi\rho + \mathbf{v}_n \cdot \mathbf{g} + \mathbf{j}_s \cdot \mathbf{v}_s, \end{aligned} \quad (4)$$

with the associated Gibbs-Duhem equation:

$$0 = -dP + sdT + w_{ik}d\lambda_{ik} + \rho d\phi + \mathbf{g} \cdot d\mathbf{v}_n + \mathbf{v}_s \cdot d\mathbf{j}_s. \quad (5)$$

In these expressions, T is the temperature, s is the entropy density, P the pressure, λ_{ik} the elastic tensor density, ϕ the chemical potential, ρ the mass density, \mathbf{v}_n the normal fluid velocity, \mathbf{g} the momentum density, \mathbf{j}_s is the superfluid momentum density, and w_{ik} is the strain tensor defined as,

$$w_{ik} = \partial_i u_k, \quad (6)$$

associated with the lattice displacement \mathbf{u} . The subscripts n, s denote normal and superfluid components respectively while i, j, k are coordinate indices. Here and in the rest of the paper summation over repeated coordinate indices is implied.

The linearized hydrodynamic equations of motion [33] are:

$$\begin{aligned} \partial_t \rho + \partial_i g_i &= 0, \\ \partial_t g_i + \partial_k \Pi_{ik} &= 0, \\ \partial_t s + \partial_i f_i &= -\frac{q_i}{T^2} \partial_i T, \\ \partial_t v_{si} + \partial_i \phi &= 0, \\ \partial_t u_i &= v_{ni}. \end{aligned} \quad (7)$$

where

$$\begin{aligned} g_i &= \rho_{sik}(v_{sk} - v_{nk}) + \rho v_{ni}, \\ \Pi_{ik} &= -\eta_{iklm} \partial_m v_{nl} - \zeta_{ik} \partial_l j_{sl} + P \delta_{ik} - \lambda_{ki}, \\ f_i &= s v_{ni} + \frac{q_i}{T}, \\ \phi &= -v_{sk} v_{nk} + \zeta_{ik} \partial_k v_{ni} + \chi \partial_k j_{sk}. \end{aligned} \quad (8)$$

These expressions can be found, with one minor [41] difference in Ref. [33]. In the expression for the momentum flux tensor (Π_{ik}) above, the tensor with components η_{iklm} is a shear viscosity arising from the normal component. On the other hand, the tensor ζ_{ik} and the scalar χ are ‘‘second viscosity’’ coefficients arising from coupling between normal and superfluid components. Also, f_i is the entropy flux and q_i is the thermal current.

Having established a framework for calculating the energy dissipation associated with dislocation motion, we now turn to the evaluation of the strain term contribution to the mobility.

2.2 Contribution of the strain term to the mobility

We now explain the procedure used to calculate the dislocation mobility. We illustrate the details by considering first the contribution to M arising from the energy dissipation E_{strain} associated with the strain field (w_{ik}) of the dislocation line. Other contributions will be discussed later. The expression for this source of energy dissipation is obtained by making use of Eqns. (4), (6) and (8):

$$\begin{aligned}\dot{E}_{strain} &= \lambda_{ik}\dot{w}_{ik} \\ &= (-\eta_{kilm}\partial_m v_{nl} - \zeta_{ki}\partial_l j_{sl} + P\delta_{ki} - \Pi_{ki})\partial_i \dot{u}_k,\end{aligned}\quad (9)$$

where the overdot denotes the time derivative. Following Ref. [32], \mathbf{u} is the displacement field of the crystal lattice sites from their equilibrium positions due to a dislocation line moving with constant velocity \mathbf{V}_D . Thus, we assume the space and time dependence of \mathbf{u} to be of the form

$$\mathbf{u}(\mathbf{r}, t) = \mathbf{u}(\mathbf{r} - \mathbf{V}_D t), \quad (10)$$

which implies

$$\partial_t \mathbf{u} = -(\mathbf{V}_D \cdot \nabla) \mathbf{u} \quad (11)$$

corresponding to the velocity of atoms moving with the dislocation line. Also, $\mathbf{v}_s = \partial_t \mathbf{u}_s(\mathbf{r} - \mathbf{V}_D t)$, is the velocity of superfluid atoms due to the moving dislocation line. Keeping the relevant dissipative terms in \dot{E}_{strain} , which lead to a V_D^2 dependence (for example in the term $\eta_{kilm}\partial_m v_{nl}\partial_i \dot{u}_k$ both v_{nl} and \dot{u}_k depend on V_D), we have:

$$\lambda_{ik}\dot{w}_{ik} = (-\eta_{kilm}\partial_m v_{nl} - \zeta_{ki}\partial_l j_{sl})\partial_i \dot{u}_k \quad (12)$$

where, $j_{sl} = \rho_{slk}v_{sk}$ and v_n are the supercurrent and the normal fluid velocity. Making then use of Eq. (2), we have for the energy dissipated in the strain field of the dislocation line:

$$\begin{aligned}F_D V_D |_{\eta, \zeta} &= - \int \dot{E}_{strain} d^2 r, \\ &= \int (\eta_{kilm}\partial_m v_{nl}\partial_i \dot{u}_k + \zeta_{ki}\partial_l j_{sl}\partial_i \dot{u}_k) d^2 r,\end{aligned}\quad (13)$$

where the notation in the left side denotes the contribution from the η and ζ tensors, under examination. We now establish a coordinate system with the z axis directed along the dislocation line and the x axis along the velocity. We then perform a two dimensional Fourier transform for the displacement field in the transverse directions:

$$\mathbf{u}(\mathbf{r}) = \int \mathbf{u}(\mathbf{q}) e^{i\mathbf{q}\cdot\mathbf{r}} d^2 q. \quad (14)$$

We illustrate below the steps involved in evaluating the inverse dislocation mobility contribution due to the shear viscosity term η_{kilm} in Eq. (13) above.

The inverse mobility contribution from the term ζ is evaluated in a very similar way. The next steps, then, involve collecting the contributions from different dissipative coefficients in Eqs. (4) and (8). Inserting the Fourier transform of the displacement field as in Eq.(14) into Eq.(13) (also using the last of Eq.(7)) we obtain

$$\begin{aligned}
F_D V_D|_\eta &= \int (\eta_{kilm} \partial_m v_{nl} \partial_i \dot{u}_k) d^2 r \\
&= \int [\eta_{kilm} \partial_m (\mathbf{V}_D \cdot \nabla) \int u_l(\mathbf{q}_1) e^{i\mathbf{q}_1 \cdot \mathbf{r}} d^2 q_1 \partial_i (\mathbf{V}_D \cdot \nabla) \int u_k(\mathbf{q}_2) e^{i\mathbf{q}_2 \cdot \mathbf{r}} d^2 q_2] d^2 r \\
&= \eta_{kilm} \int \int i q_{1m} (i \mathbf{V}_D \cdot \mathbf{q}_1) u_l(\mathbf{q}_1) e^{i\mathbf{q}_1 \cdot \mathbf{r}} d^2 q_1 \times \\
&\quad \int i q_{2i} (i \mathbf{V}_D \cdot \mathbf{q}_2) u_k(\mathbf{q}_2) e^{i\mathbf{q}_2 \cdot \mathbf{r}} d^2 q_2 d^2 r. \tag{15}
\end{aligned}$$

Noting that the integral over the 2D plane leads to a two-dimensional $\delta(\mathbf{q}_1 + \mathbf{q}_2)$ and using this delta function to integrate over \mathbf{q}_2 one then obtains

$$F_D V_D|_\eta = \eta_{kilm} \int q_{1m} q_{1i} u_l(\mathbf{q}_1) u_k(-\mathbf{q}_1) (V_D^2 q_{1x}^2) d^2 q_1. \tag{16}$$

To estimate this contribution to the mobility it is sufficient to consider the diagonal component of the viscosity, the ordinary $\eta \equiv \eta_{iiii}$. Then, the rate of energy loss in the strain field of a dislocation line simplifies to:

$$F_D V_D|_\eta = \eta \int q_{1i} q_{1i} u_i(\mathbf{q}_1) u_i(-\mathbf{q}_1) (V_D^2 q_{1x}^2) d^2 q_1. \tag{17}$$

By simplifying the equation above and finding the inverse mobility of the dislocation line as explained after Eq.(3) we obtain for this contribution to M^{-1} :

$$M^{-1}|_\eta = \eta \int_{q_{min}}^{q_{max}} q_{1i}^2 |u_i(\mathbf{q}_1)|^2 q_{1x}^2 d^2 q_1 \tag{18}$$

where $q_{min} = 1/L$, L being a cutoff of order of the size of the crystal, or the distance between dislocations, and $q_{max} = 1/b$ with b (the magnitude of Burgers vector) approximately comparable to the interatomic spacing. To obtain $\mathbf{u}(\mathbf{q})$, (the Fourier transform of the elastic displacement field) we note that the gradient of the elastic displacement field is roughly constant in magnitude over a circular path of radius r centered on the dislocation line [32] i.e.

$$(\nabla u)r \approx b. \tag{19}$$

Fourier transforming the elastic displacement field then leads to:

$$u(\mathbf{q}) \approx \frac{b}{q^2}. \tag{20}$$

Substituting Eq. (20) into Eq. (18) we finally have:

$$M^{-1}|_\eta = \frac{\eta}{2} \left(1 - \frac{b^2}{L^2}\right) \sim \frac{\eta}{2}. \tag{21}$$

since obviously $b \ll L$.

As mentioned above, in addition to this term arising from η , which we have discussed in detail, and the corresponding contribution from the ζ tensor, written down in Eq. (13) and computed in the same way as the η term, there are several additional contributions to the dissipation all arising from terms in Eq. (4). We can ignore the contribution from the $T\dot{S}$ because we are interested in the limit where $T \rightarrow 0$. Also, since we are interested in the limit where V_D is small compared to the speed of sound (in solid ^4He) the inertial contribution to energy dissipation, $\mathbf{v}_n \cdot \dot{\mathbf{g}}$, can be neglected [32]. There are additional contributions to the mobility of the dislocation line arising from the $\phi\dot{\rho} + \mathbf{j}_s \cdot \dot{\mathbf{v}}_s$ terms in Eq. (4). These involve again the tensor ζ , this time via the last of Eqs. (8) and also, via the same equation, the scalar χ . These contributions can be calculated following similar procedures to those discussed above and there is no need to repeat the details. Finally, putting together all of these contributions, the total inverse mobility of the dislocation line in a quantum crystal can be written as

$$M^{-1} \approx \frac{\eta}{2} + \frac{\rho_s}{\rho}(\zeta\rho + \chi\rho^2). \quad (22)$$

This is our basic result for the mobility.

2.3 Relation between shear modulus and mobility

We will now proceed further to relate the observed shear modulus of a quantum crystal to the mobility of a dislocation line. This will enable us to discuss the experimental results of Ref. [11].

When a stress σ is applied to a crystal, the dislocation line feels a force per unit length, $F_D = b\sigma$. As the dislocation line glides in response to the applied force, the displacement of the dislocation line results of course in a strain ϵ_D in addition to the strain ϵ_{el} . Here the elastic strain ϵ_{el} is the response of the crystal in the absence of dislocation lines. Therefore, the effective shear modulus μ i.e. the ratio of applied stress to total strain is given by [11] $\mu = \sigma/(\epsilon_D + \epsilon_{el})$. This can also be written as

$$\mu = \frac{\mu_{el}}{1 + \frac{\epsilon_D}{\epsilon_{el}}}, \quad (23)$$

where $\mu_{el} = \sigma/\epsilon_{el}$ is the elastic shear modulus. The strain due to the motion of the dislocation line is known to be [42, 43]

$$\epsilon_D = \rho_D b x_a, \quad (24)$$

where ρ_D is the dislocation number density and x_a is the average displacement of the dislocation line through the crystal. In order to determine the dislocation displacement, we look to the applicable equation of motion [44] of the dislocation line

$$M^{-1}\dot{x} = b\sigma. \quad (25)$$

where x is the dislocation displacement as a function of time. We can then relate the average displacement of the dislocation to its velocity and to mobility via $x_a = V_D \tau$ (where τ is the characteristic time scale associated with the movement of the dislocation line) and Eq. (1) to obtain $\epsilon_D = F_D \rho_D b M \tau$, which agrees with Eq. (25) and $F_D = b\sigma$. For the purposes of estimating the the average displacement x_a , we will, working as in Ref. [37] in the quasistatic limit, replace τ by the inverse of the slowest range of frequencies for the strain ϵ applied to the crystal in the experimental [11] situation.

Putting together these considerations, the shear modulus of the crystal as a function of the mobility of the dislocation line is found to be

$$\mu = \frac{\mu_{el}}{1 + \frac{F_D \rho_D b M \tau}{\epsilon_{el}}} \quad (26)$$

We will now be able to use this result, combined with that for the mobility in the previous subsection (Eq. (22)) to discuss the behavior of the elastic coefficient in solid Helium.

The expressions derived above for the amplitude of displacement and ϵ_D are valid under the standard [36,37] quasistatic limit assumptions. This is applicable in the experimental situation since the dislocation acceleration time is small compared to the time over which strain is applied to the crystal [45]. However, we can also consider the higher frequency limit (the ‘‘ac’’ limit) when the dislocation line executes elastic string motion out of phase with the applied strain. Considering then, $x(t) = x_0 e^{-i\omega t}$ and $\sigma(t) = \sigma_0 e^{-i\omega t}$ one obtains from Eq.(25):

$$x_0 = \frac{ib\sigma_0}{M^{-1}\omega}. \quad (27)$$

Following then the same steps as in the previous case we can easily find $\mu(\omega)$ in this ‘‘ac’’ limit. The quantity of interest here is the Q factor $|Q^{-1}| = |Im[\mu]/Re[\mu]|$. Defining $\epsilon_R(\omega) \equiv \frac{\rho_D b F_D M^*(1/\omega)}{\epsilon_{el}}$ as a ratio involving strains, one finds that $Im[\mu] = -\epsilon_R Re[\mu]$, leading to the expression for the Q factor, $|Q^{-1}| = |Im[\mu]/Re[\mu]| = \epsilon_R(\omega)$.

3 Results - Modeling of Experimental Shear Modulus Data

Having derived the mobility of the dislocation line and its relation to the shear modulus of a quantum crystal, we now discuss how to connect our theory to the experimentally observed large and sudden softening of the shear modulus seen [11] in solid ^4He as the temperature is increased. Thus, we will seek to model the temperature dependence of the shear modulus data. Results in Ref. [11] show that at the higher temperatures studied, (up to 1K), the crystal is softer, with μ being independent of temperature. As the temperature is lowered, it is seen that between $T = 0.05\text{K}$ and 0.1K μ rises sharply, and then, at lower temperatures, it saturates to a value identified with the intrinsic value μ_{el} . It is evident from earlier studies [34,35] that dislocation lines play

an important role in determining the elastic properties such as shear modulus of a crystal. Pinning due to impurity atoms and collision with thermal phonons have been considered to be the dominant source for damping of dislocation line motion in recent experiments [31,30]: hence we have to compare these sources of damping with the superfluid contribution in order to ascertain their relative importance. In ^4He crystals, dislocation lines can glide almost freely along the basal planes of the hexagonal crystal structure [31]. As a consequence, the effect of the shear viscosity (i.e. the dissipation due to η , arising from interactions between the dislocation line and the surrounding atoms) can be neglected. It follows from the above argument that the expression for the dislocation mobility, Eq. (22) then simplifies to:

$$M^{-1} \approx \frac{\rho_s}{\rho} (\zeta\rho + \chi\rho^2). \quad (28)$$

An important consequence of this result is that a superfluid field makes it harder for the dislocation line to move. Since the inverse mobility is directly proportional to the superfluid fraction, at lower temperatures (as $T \rightarrow 0$) when we expect ρ_s/ρ to be larger, it is harder for the dislocation line to move. Even though this appears to be counterintuitive, it can be understood by recalling that Couette viscometer [46] and vibrating wire [47] experiments show that liquid ^4He is characterized by a very small viscosity of order 10^{-5} kg/ms below 1K. This is relevant because the small viscosity contribution from the superfluid field could be the dominant source of dissipation for a dislocation line in a quantum solid.

We can now numerically estimate the inverse mobility of the dislocation line. To do so, we will use the values of the second viscosity coefficients $\rho\zeta \sim 10^{-5}$ kg/ms and $\rho^2\chi \sim 7 * 10^{-5}$ kg/ms for liquid ^4He [48,49]. These coefficients are not known for solid ^4He . We will then obtain corresponding estimates for the dislocation mobility both above and below the assumed superfluid transition temperature (or crossover) in solid ^4He crystals. For the purposes of estimating the temperature at which a superfluid field associated with dislocations may arise in solid ^4He crystals, we consider a scenario where a loosely intersecting grid of dislocations forms. According to Refs. [50,18] dislocation network superfluidity is characterized by two temperature scales - $T_0 \sim 1\text{K}$ (comparable to the bulk λ temperature for liquid ^4He) and $T_c \sim T_0 a/L_f$, where a is the interatomic distance along a dislocation core and L_f is the free segment length of dislocation line. Within such a model for superfluidity associated with dislocation lines, the onset temperatures are roughly consistent with the experimentally [11,51,52] found range 0.1K to 0.075K where the onset of anomalous behavior is observed. As to the numerical value of the putative superfluid fraction ρ_s/ρ we look to quantum Monte Carlo calculations involving solid ^4He . Monte Carlo simulations with dislocations characterized by core superfluidity find that nearly all atoms in the core of a dislocation line are in the superfluid state [15]. We will conservatively take the value $\rho_s/\rho \sim 0.1$ in the $T \rightarrow 0$ limit for the superfluid fraction near the dislocation core. It is very easy to see that for any reasonable values of the dislocation density in solid

^4He crystals [29], and of the radius from the dislocation core in which superfluidity might be present, this estimate of the superfluid density near the core leads to a superfluid fraction averaged over the whole sample well below the current experimental upper limit for $\rho_s/\rho \sim 10^{-6}$ [53]. Monte Carlo studies of superfluidity associated with dislocation lines focus on whether a fully connected three-dimensional network of superfluid flow is established as a possible explanation to the purported observation of period drop in torsion oscillator experiments. In this context, it is found [54] that edge dislocations can display finite superfluid response. Other simulations [19] consider a temperature range (0.5 K) much higher than what is relevant here.

Using these order of magnitude values we can obtain, via Eq. (28), an approximate value for the inverse mobility (M^{-1}) at low T namely $\sim 10^{-5}$ kg/ms. In some of the previous work, [55] damping of dislocation motion was thought to be mainly due to phonon collisions and pinning effect due to the presence of ^3He impurities, resulting in inverse mobilities of order 10^{-9} kg/ms and 10^{-8} kg/ms, respectively, at 1K. Hence, our results indicate that quenching of dislocation motion due to superfluid field may be the dominant source of damping for dislocation motion in the low temperature limit. In this limit, the superfluid contribution to dislocation damping is larger by at two or three orders of magnitude compared to the other sources of damping.

In order to estimate the magnitude of the shear modulus using Eq. (26), (with Eq. (28)), we need also the relevant values of the other parameters entering that equation. From experimental results [31, 11, 29], we have $F_D \sim 10^{-11}$ N/m, $\rho_D \sim 10^6$ m $^{-2}$, $b \sim 10^{-10}$ m and $\epsilon_{el} \sim 10^{-8}$. As mentioned above, we use the inverse of the applied frequency, in the low range, $\omega \sim 1$ Hz - 50 Hz, to estimate τ . This should be better at lower frequencies. Inserting the values of the various parameters into Eq. (26) and taking $M^{-1} \sim 10^{-5}$ kg/ms in the low T limit as mentioned above, we obtain the ratio in the denominator of that equation to be

$$\frac{F_D \rho_D b M \tau}{\epsilon_{el}} \sim 10^{-3} - 10^{-5}. \quad (29)$$

It can then be easily seen from Eq. (26) that $\mu \approx \mu_{el}$ in the low T regime. Thus, at low temperatures (below $T \sim 0.03$ K), we find that the shear modulus becomes independent of T at $\mu \approx \mu_{el}$, a result that should not depend on frequency at low ω . In comparing the experimental results for the shear modulus with our model (see Fig.1), we note that the low temperature behavior of this shear modulus is well accounted for in our theory.

Examining now the behavior of the dislocation mobility near and above the temperature where the assumed superfluid behavior disappears, we note that the contribution to the inverse mobility due to the superfluid field approaches zero as $\rho_s/\rho \rightarrow 0$. Then, other damping effects such as pinning due to ^3He impurities and phonon scattering should become more important and eventually dominant. The experimental range of temperatures where the sharp change in shear modulus is found in solid ^4He (as mentioned above), is accounted for in our theory. In order to estimate the shear modulus in the higher temperature

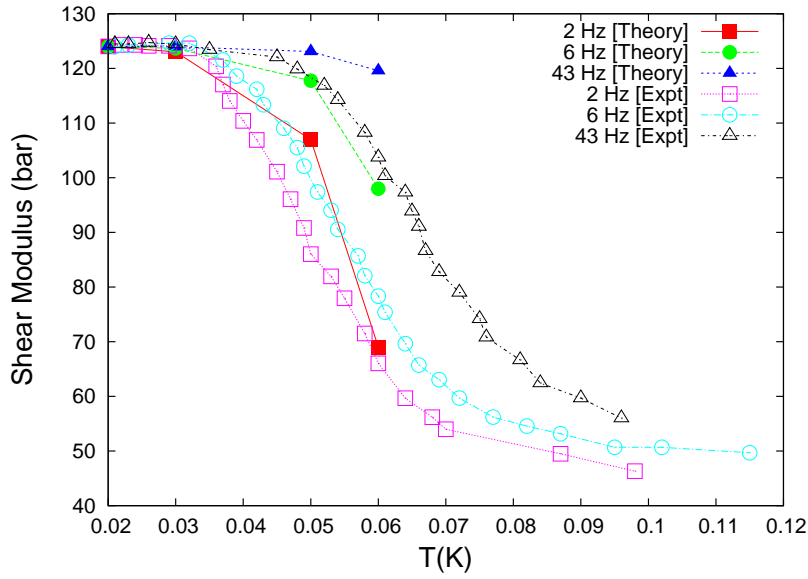


Fig. 1 (Color online) Experimental results from Ref. [11] for the shear modulus vs temperature at different frequencies, ω , of applied strain (see legend) are compared with theoretical results. See text for discussion.

range ($T \geq 0.03\text{K}$) we first note [11, 31] that $M^{-1} \sim 10^{-8}$ kg/ms at $T = 0.06\text{K}$. This implies that the ratio in Eq. (29) is of order unity and $\mu \approx 0.5\mu_{el}$. At the intermediate value $T = 0.05\text{K}$ we interpolate $M^{-1} \sim 5 \cdot 10^{-7}$ kg/ms. At lower T the precise value of M^{-1} becomes irrelevant. The results thus obtained are displayed in Fig. 1. Other parameter values used there are, except of course for ρ_s , the same as in the low temperature range. As shown there, the drop in shear modulus is modeled quite well by Eq. (26) and the above considerations, specially at the lowest frequencies. In the higher frequency range considered the quasistatic approximations might start to break down. We also note that at a given temperature, as the frequency ω is lowered the value of the shear modulus decreases in agreement with experimental data.

Considering now the higher frequency “ac” limit, we focus, as mentioned above, on the Q factor. In Fig. 2, we plot the dissipation associated with dislocation line vibration, Q^{-1} (i.e. arising from the phase difference between σ and ϵ) as obtained from $|Q^{-1}| = \epsilon_R$. (see discussion at the end of Sec. 2.3). Dissipation is small at low temperatures and increases with T . The numerical values of the parameters used in calculating Q^{-1} are the same as for the shear modulus. The experimental results [11, 30] for Q^{-1} in the low T limit are again consistent with theory: the disagreement is now greater at very low frequencies, as one would expect. At temperatures near the superfluid onset temperature, we note that experimentally the dissipation decreases with larger values of ω . This frequency behavior of the dissipation is in agreement with our results.

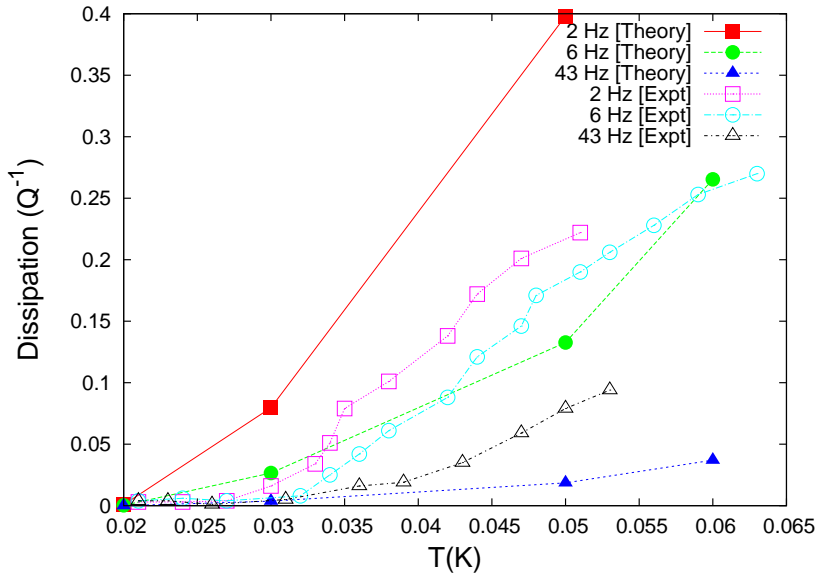


Fig. 2 (Color online) Dissipation (Q^{-1}) vs temperature at different frequencies, ω , of applied strain (legend). Experimental data from Ref. [11] are compared with theory, as discussed in the text.

Next, we discuss some of the limitations of our model. First, the calculated dislocation mobility in the hydrodynamic limit provides probably a lower limit to this quantity since we do not take into account the core strain effects of the dislocation line. Also, as noted above, the second viscosity coefficients used in calculating the mobility are for liquid ${}^4\text{He}$ rather than for solid ${}^4\text{He}$, due to the lack of experimental data in the solid phase. Since one might reasonably expect the second viscosity coefficients for solid ${}^4\text{He}$ to be somewhat larger than in the liquid, it is possible that even for smaller ratios of ρ_s/ρ than the value $\rho_s/\rho \sim 0.1$ considered here the superfluid contribution to the dislocation mobility could still be significant compared to the contribution from phonon scattering or pinning effects due to impurities. These reasons, then, might account for the remaining differences in the magnitude of the temperature dependence of the shear modulus and dissipation as shown in Figs. 1 and 2. The onset temperature for shear modulus softening was observed to increase with increasing ${}^3\text{He}$ impurity concentration [6]. This behavior can be qualitatively understood from our ideas: we have shown that a model [26] of a dislocation network with quenched disorder has a higher ordering temperature than in the annealed case. Higher impurity concentration would be more effective in quenching the dislocation network thereby increasing the onset temperature of the superfluid field. More detailed knowledge of the phonon and impurity effects is thus, we believe, likely to lead to a more quantitative agreement in the higher T limit. In our comparison with experiment, we have implicitly assumed that the dislocations with superfluid cores couple to the measured

shear modulus. Our mobility estimates can be applied to all dislocations. The arguments given above in the context of estimating the superfluid fraction and MC results indicate that our assumption appears justified.

4 Summary

We have begun, in section 2.1 of this paper, by presenting a novel calculation of the dislocation mobility in solid ^4He . This calculation is based on well known hydrodynamic results [33] and follows a procedure developed in Ref. [32]. The result is expressed in terms of the bulk “second viscosities” of the superfluid crystal hydrodynamics, and the value of ρ_s , assumed to be nonzero. Numerical estimates of the mobility, although rather uncertain, indicate that a putative superfluid field associated with dislocation lines, can play a nontrivial role in dislocation mobility and therefore affect the stiffness of the crystal. We show that as a consequence, superfluid damping of dislocation motion can model the large and sudden increase in shear modulus observed experimentally in solid ^4He as the temperature is decreased, as seen in Fig. 1. At low temperatures, below 200mK, solid ^4He crystals stiffen considerably. This is thought to be due to pinning of dislocation network by ^3He impurities and damping of dislocation motion due to phonon collisions. Within our assumptions, however, we find that as the superfluid fraction increases at lower temperatures the dislocation mobility decreases resulting in the stiffening of the crystal. Numerical estimates of the change in shear modulus and the Q factor based on this effect model the experimental behavior quite well, as can be seen from the figures. The quantitative agreement might be even better when it is taken into account that bulk viscosities of solid ^4He are likely be larger than the values for liquid ^4He used in the mobility estimates. We have used the known values of these quantities for the liquid, as information for their values in the solid is lacking.

Our results then show that quenching of dislocation motion due to a superfluid field could be an important source, even possibly the dominant one, of damping for dislocation motion in clean crystals at the low temperature limit. In this limit (i.e. $T \leq 0.04K$), we find that the superfluid contribution to dislocation damping is likely to be considerably larger than that due to other sources of damping (phonons and impurity pinning). The superfluid contribution would dominate because, experimentally, it is seen that limitation of dislocation motion in conventional crystals due to Peierls barrier is absent in solid ^4He . The onset temperature of this unusual elastic behavior in solid ^4He is in the same temperature range as the onset of superfluid behavior in [50, 18] dislocation networks. As noted above, the superfluid contribution to dislocation mobility scales with the superfluid fraction i.e. ρ_s/ρ . The onset temperature of the superfluid fraction is reflected, in our model, in the temperature dependence of the shear modulus effect. This enables us to fit both the magnitude and the temperature dependence of the change in shear modulus of solid ^4He crystal. However, at higher temperatures, the factor ρ_s/ρ becomes smaller and eventually approaches zero. In that range, other contributions to

damping (chiefly due to ^3He impurities and also phonon collisions) will become more important. Therefore, we believe that the interplay of these effects - superfluid field, ^3He impurities and phonon collisions - should be considered in understanding the anomalous softening of the ^4He crystal.

Acknowledgements This research was supported in part by IUSSTF grant 94-2010.

References

1. J.H. Hetherington. Phys. Rev. **176**, 231 (1968).
2. A.F. Andreev and I.M. Lifshitz. Sov. Phys. JETP, **29**, 6 (1969).
3. E.Polturak and N.Gov, Contemporary Physics 44, No.2, 145-151, (2003).
4. E. Kim and M.H.W. Chan. Nature (London) **427**, 225 (2004).
5. A.S.C. Rittner and J.D. Reppy. Phys. Rev. Lett. **98**, 175302 (2007).
6. J. Day and J. Beamish. Nature (London) **450**, 853 (2007).
7. J. Day, O. Syshchenko and J. Beamish. Phys. Rev. B **79**, 214524 (2009).
8. D.Y. Kim and M.H.W. Chan. Phys. Rev. B **90**, 064503 (2014).
9. I. Iwasa. Phys. Rev. B **81**, 104527 (2010).
10. I. Iwasa. J. Low Temp. Phys. **171**, 287 (2013).
11. A.D. Fefferman, F. Souris, A. Haziot, J.R. Beamish and S. Balibar. Phys. Rev. B **89**, 014105(2014).
12. C. Zhou, J-J. Su, M.J. Graf, C. Reichhardt, A.V. Balatsky, I.J. Beyerlein. Philos. Mag. Lett. **92** (11), 608-616 (2012).
13. C. Zhou, J-J. Su, M.J. Graf, C. Reichhardt, A.V. Balatsky, I.J. Beyerlein. Phys. Rev. B **88**, 024513 (2013).
14. A.B. Kuklov, L. Pollet, N.V. Prokof'ev and B.V. Svistunov. Phys. Rev. B **90**, 184508 (2014).
15. M. Boninsegni, A. B. Kuklov, L. Pollet, N. V. Prokof'ev, B. V. Svistunov, and M. Troyer. Phys. Rev. Lett. **99**, 035301 (2007).
16. L. Pollet, M. Boninsegni, A. B. Kuklov, N. V. Prokof'ev, B. V. Svistunov, and M. Troyer. Phys. Rev. Lett. **98**, 135301 (2007).
17. Y. Vekhov, R.B. Hallock. Phys. Rev. B **91**, 180506(R) (2015).
18. D. Aleinikava, E. Dedits and A.B. Kuklov. J Low Temp Phys. **162**: 464-475 (2011).
19. Ş. G. Söyler, A. B. Kuklov, L. Pollet, N. V. Prokof'ev, and B. V. Svistunov, Phys. Rev. Lett. **103**, 175301(2009).
20. S. Balibar, J. Beamish, and R.B. Hallock, J. Low Temp. Phys, **180**, 3 (2015).
21. R. B. Hallock, J. Low Temp. Phys, **180**, 6 (2015).
22. A.B. Kuklov, Phys. Rev. B **90**, 184508 (2014).
23. H. Choi, D. Takahashi, K. Kono, E. Kim, Science **330**, 1512 (2010).
24. H. Choi, D. Takahashi, K. Kono, E. Kim, Phys. Rev. Lett. **108**, 105302 (2012).
25. J. Toner. Phys. Rev. Lett. **100**, 035302 (2008).
26. A. N. Malmi-Kakkada, O.T. Valls and C. Dasgupta. Phys. Rev. B. **90**, 024202 (2014).
27. F. Souris, A.D. Fefferman, A. Haziot, N. Garroum, J.R. Beamish and S. Balibar. J. Low Temp. Phys. **178**, 149-161 (2015).
28. X. Rojas, C. Pantalei, H.J. Maris and S. Balibar. J. Low Temp. Phys. **158**, 478-484 (2010).
29. X. Rojas, A. Haziot, V. Bapst, S. Balibar and H.J. Maris. Phys. Rev. Lett. **105**, 145302 (2010).
30. A. Haziot, A.D. Fefferman, F. Souris, J.R. Beamish and S. Balibar. Phys. Rev. Lett. **110**, 035301(2013).
31. A. Haziot, A.D. Fefferman, F. Souris, J.R. Beamish and S. Balibar. Phys. Rev. B **87**, 060509 R(2013).
32. T.C. Lubensky, S. Ramaswamy and J. Toner. Phys. Rev. B **33**, 11 (1986).
33. W.M. Saslow. Phys. Rev. B **15**, 173 (1977); J. Low Temp. Phys. **169**, 248-263 (2012).
34. H. Suzuki. J. Phys. Soc. Jpn. **35**, 1472 (1973).

35. H. Suzuki. *J. Phys. Soc. Jpn.* **42**, 1865 (1977).
36. J. A. Gorman, D. S. Wood and T. Vreeland, Jr. *J. Appl. Phys.* **40**, 2 (1969).
37. J. Day, O. Syshchenko and J. Beamish. *Phys. Rev. Lett.* **104**, 075302 (2010).
38. O. Syshchenko, J. Day and J. Beamish. *Phys. Rev. Lett.* **104**, 195301 (2010).
39. G.N. Lazareva and A.S. Bakai. *J. Phys.:Condens. Matter* **21**, 295401 (2009).
40. C. Dasgupta and O.T. Valls, *Phys. Rev. E* **79**, 016303 (2009).
41. The first of Eqs. (8) differs slightly from the corresponding expression in the first of Ref. [33]. That expression contains a small error, which we are very grateful to Prof. Saslow for pointing out to us.
42. G.I. Taylor. *Proc. R. Soc. Lond. A* **145**, 362 (1934).
43. E. Orowan. *Proc. Phys. Soc.* **52**, 8 (1940).
44. A. Granato and K. Lucke. *J. Appl. Phys.* **27**, 583 (1956). We consider the limit whereby the effective mass per unit length as well as the effective tension per unit length of the dislocation line is negligible.
45. The acceleration time constant is given by the ratio of mass per unit length to the inverse mobility of the dislocation line. This time constant is very small $\sim 10^{-13}$ sec.
46. A. D. B. Woods and A. C. Hollis Hallett. *Can. J. Phys.* **41**, 596-609 (1962).
47. J. T. Tough, W. D. McCormick, and J. G. Dash. *Phys. Rev.* **132**, 2373-2378 (1963).
48. S. Putterman. *Phys. Rev. Lett.* **26**, No. 8 (1971).
49. C-I Um. Technical Report - Office of Naval Research (1992).
50. S.I. Shevchenko, *Sov. J. Low Temp. Phys* **14**, 553 (1988).
51. M. H. W. Chan, K. I. Blum, S. Q. Murphy, G. K. S. Wong, J. D. Reppy. *Phys. Rev. Lett.* **61**, 1950(1988).
52. E. Kim and M. H. W. Chan. *Nature* **427**, 225 (2004).
53. D.Y. Kim and M.H.W Chan. *Phys. Rev. B* **90**, 064503(2014).
54. M. Boninsegni, N.V. Prokof'ev, *Rev. Mod. Phys.* **84**, 759 (2012).
55. A. Haziot, A.D. Fefferman, F. Souris, J.R. Beamish and S. Balibar. *Phys. Rev. B* **88**, 014106(2013).